Article

Metoprolol Inhibits Developmental Brain Sterol Biosynthesis in Mice

Luke B. Allen [1,2] **and Károly Mirnics** [1,2,3,4,*]

1   Munroe-Meyer Institute for Genetics and Rehabilitation, University of Nebraska Medical Center, Omaha, NE 68105, USA
2   Department of Biochemistry and Molecular Biology, College of Medicine, University of Nebraska Medical Center, Omaha, NE 68198, USA
3   Department of Pharmacology and Experimental Neuroscience, College of Medicine, University of Nebraska Medical Center, Omaha, NE 68198, USA
4   Department of Psychiatry, College of Medicine, University of Nebraska Medical Center, Omaha, NE 68198, USA
*   Correspondence: karoly.mirnics@unmc.edu

Abstract: De novo sterol synthesis is a critical homeostatic mechanism in the brain that begins during early embryonic development and continues throughout life. Multiple medications have sterol-biosynthesis-inhibiting side effects, with potentially detrimental effects on brain health. Using LC-MS/MS, we investigated the effects of six commonly used beta-blockers on brain sterol biosynthesis in vitro using cell lines. Two beta-blockers, metoprolol (MTP) and nebivolol, showed extreme elevations of the highly oxidizable cholesterol precursor 7-dehydrocholesterol (7-DHC) in vitro across multiple cell lines. We followed up on the MTP findings using a maternal exposure model in mice. We found that 7-DHC was significantly elevated in all maternal brain regions analyzed as well as in the heart, liver and brain of the maternally exposed offspring. Since DHCR7-inhibiting/7-DHC elevating compounds can be considered teratogens, these findings suggest that MTP utilization during pregnancy might be detrimental for the development of offspring, and alternative beta-blockers should be considered.

Keywords: beta-blockers; LC-MS/MS; 7-DHC; DHCR7; desmosterol; cholesterol; nebivolol; propranolol; atenolol; cell culture; neuron; astrocyte

1. Introduction

Cholesterol is an essential molecule of life and is particularly important for brain development and function [1]. Although the human brain only accounts for about 2% of the total body weight, it contains as much as 25% of the cholesterol and cholesterol derivatives in the body [2–4]. The developing brain begins synthesizing its own cholesterol during embryonic development [3–6]. Cholesterol in the central nervous system (CNS) functions as much more than a structural component of cellular membranes and lipid rafts: it is required for synapse and dendrite formation as well as axonal guidance, and it serves as a precursor for various biosynthetic pathways [7–9].

The last step in the Kandutsch–Russell arm of the cholesterol biosynthesis pathway is the conversion of 7-dehydrocholesterol (7-DHC) to cholesterol, catalyzed by a single enzyme, 7-dehyrocholesterol reductase (DHCR7) (Figure S1) [10]. DHCR7 inhibition leads to reduced levels of cholesterol and desmosterol (DES)—cholesterol's precursor in the Bloch sterol biosynthesis pathway—and accumulation of their immediate precursors, 7-DHC and 7-dehyrodesmosterol (7-DHD) [11–14]. 7-DHC and 7-DHD are the most reactive lipids known to date with a propagation rate constant of 2160 (this is 200-times more than cholesterol and 10-times more than arachidonic acid) [11].

This results in the formation of highly reactive autoxidation sterols, called 7-DHC-derived oxysterols [15–17]. These 7-DHC-derived oxysterols are reactive electrophiles that

impair cell viability, differentiation, and growth [18–20]. They are not only markers of oxidative stress but are also biologically potent compounds capable of impeding or altering immune function [21]. In addition, DHCR7 inhibitors, which elevate 7-DHC levels and reduce DES levels during pregnancy are considered teratogens [22]. Finally, two mutant copies of the DHCR7 gene are either lethal (if sterol synthesis is fully eliminated) or result in a severe developmental disability called Smith-Lemli-Opitz syndrome (if some amount of residual cholesterol synthesis is preserved) [23–25].

As the blood–brain barrier (BBB) prevents passage of cholesterol from the rest of body to the central nervous system, the brain fully relies on its own cholesterol biosynthesis [6]. However, a significant number of medications with sterol biosynthesis inhibiting side effects can and do cross BBB—including haloperidol, aripiprazole, cariprazine, buspirone, trazodone, and others [26–33]. Our preliminary, high-throughput screening data on Neuro2a cells data suggested that commonly used beta-blockers for treatment of cardiovascular disease that pass through the BBB may interfere with normal sterol biosynthesis through off-target effects on the DHCR7 enzyme [34–36].

Chronic and gestational hypertension are the most common disorders of pregnancy and can result in premature birth [37]. Both are treated in order to prolong pregnancy and maximize the gestational age of the infant [38]. At the same time, maternal exposure to medications must be considered to avoid potential adverse effects on the developing fetus. The utilization of antihypertensive drugs during pregnancy, and the potential effect on the developing fetus have been topics of considerable debate: some studies found no negative effect on fetal development [39,40], while others reported increased risk for intrauterine growth restriction, small for gestational age, and preterm delivery [41–43]. As a result, we embarked on assessing the effects of six commonly used beta-blockers on sterol biosynthesis, utilizing cell lines, neuronal and astroglial cultures, and an in vivo mouse model.

2. Materials and Methods

2.1. Chemicals

Unless otherwise noted, all chemicals were purchased from Sigma-Aldrich Co (St. Louis, MO, USA). HPLC-grade solvents were purchased from Thermo Fisher Scientific Inc. (Waltham, MA, USA). All sterol standards, natural and isotopically labeled, used in this study are available from Kerafast, Inc. (Boston, MA, USA).

2.2. Cell Line Cultures

Human hepatocellular carcinoma HepG2 cells and the mouse neuroblastoma cell line Neuro2a, were purchased from ATCC (Rockville, MD, USA). The human and mouse cell lines were maintained in EMEM supplemented with L-glutamine, 10% FBS, and puromycin at 37 °C and 5% CO_2. Cells were subcultured once a week and the culture medium changed every 2 days. For experimental purposes, the cells were plated in 96-well plates (for cell viability and sterol analysis).

To assess the endogenous sterol synthesis, these cultures were grown in defined medium without cholesterol and without lipids by using EMEM with N2 supplement and L-glutamine. At the endpoint of the incubation, Hoechst dye was added to all wells in the 96-well plate and the total number of cells counted using an ImageXpress Pico and cell counting algorithm in CellReporterXpress. After removing the medium, wells were rinsed twice with 1× PBS and then stored at −80 °C for lipid analysis. All samples were analyzed within 2 weeks of freezing.

2.3. Primary Neuronal Cultures

Primary cortical neuronal cultures were prepared from E15 and E17 mice as previously described [19,44,45]. Briefly, the brain was placed in pre-chilled HBSS solution (without Ca^{2+} or Mg^{2+}), and two cortices were dissected and cut with scissors into small chunks of similar sizes and transferred to Trypsin/EDTA (0.5%) for 25 min at 37 °C. Trypsin was

removed and residual trypsin inactivated by adding Trypsin Inhibitor (Sigma T6522) for 5 min. Solution was removed, and small tissue chunks were resuspended in Neurobasal medium (NBM) with B-27 supplement (Gibco #17504–044).

Samples were then spun at $80\times g$, the pelleted tissue was resuspended in NBM with B-27 supplement and then triturated with a fire-polished Pasteur pipette. The cells were pelleted by centrifugation for 5 min at $80\times g$. The cell pellet was resuspended in NBM with B-27 supplement and the cells were counted. The cells were plated on poly-D-lysine coated 96-well plates at 60,000 cells/well. The growth medium was NBM with B-27 supplement, Glutamax and 3 μM cytosine arabinoside. Cells were incubated at 37 °C, 5% CO_2 for 6 days.

At the endpoint of the incubation, Hoechst dye was added to all wells in the 96-well plate, and the total number of cells counted using an ImageXpress Pico and cell counting algorithm in CellReporterXpress. After removing the medium, wells were rinsed twice with $1\times$ PBS and then stored at −80 °C for sterol analysis. All samples were analyzed within 2 weeks of freezing. For the current study we prepared three independent preparations of primary cortical neurons from E15 (ATN, CRV, LAB, PRO) and E17 (MTP, NEB). Previous studies by our group have shown that different embryonic preparations do not respond differently to drugs other than inherent difference in the absolute level of sterols [45]. The results were concordant for cultures obtained from both embryonic stages.

2.4. Primary Astroglia Cultures

After plating the required number of cells for neuronal cultures, left-over cells were plated in 100 mm dishes at density of 1×10^7 per tissue culture plate in DMEM with 10% FBS. Under these conditions, astrocytes adhere and divide and completely populate the plate within 10–14 days. Once the plates were full, they were rinsed using the cold jet method [46]. The astrocytes were trypsinized and plated in 96-well plates in DMEM plus 10% FBS at 30,000 cells/well. The following day, the medium was completely changed, and astrocytes were grown in Neurobasal medium with B-27 supplement in the absence of cholesterol (same medium as neuronal cells without cytosine arabinoside). Cells were incubated at 37 °C, 5% CO_2 for 6 days. At the endpoint of the incubation, cells were counted as described for neuronal cultures and processed in a similar manner for the analysis as neuronal cultures.

2.5. Mouse Studies

Adult male and female C57BL/6J stock # 000.664 mice were purchased from Jackson Laboratories. Mice were housed under a 12 h:12 h light-dark cycle at constant temperature (25 °C) and humidity with ad libitum access to food (Teklad LM-485 Mouse/Rat Irradiated Diet 7912) and water in Comparative Medicine at the UNMC, Omaha, NE. The time-pregnant female mice received IP injections of vehicle (VEH) or MTP (35 mg/kg) from E12 to E19. The mice were monitored daily during injections and E19 offspring were collected at least 2 h after the final injection of either VEH or MTP.

Adult female mice were also sacrificed at the same time as pups. Frozen brain tissue samples were sonicated in ice-cold PBS containing butylated hydroxytoluene (BHT) and triphenylphosphine (PPh_3). The aliquots of homogenized tissue were used for sterol extraction and protein measurements. The protein was measured using Pierce's BCA assay. All procedures were performed in accordance with the Guide for the Humane Use and Care of Laboratory Animals. The use of mice in this study was approved by the Institutional Animal Care and Use Committee of UNMC.

2.6. Cell Sterol Measurements

Sterol levels were analyzed in individual wells of 96-well plate, and, for most experiments, cellular levels correspond to 4–8 technical replicates. After rinsing plates with $1\times$ PBS (or removing previously frozen plates from −80 °C freezer) 200 μL of MeOH containing the internal standard cocktail was added, as reported previously [45,47]. The plate was covered by aluminum foil and then placed on an orbital shaker for 30 min at room

temperature. An aliquot (100 μL) of the supernatant was transferred to a plate predeposited with 200 μg of 4-phenyl-1,2,4-triazoline-3,5-dione (PTAD) and sealed with Easy Pierce Heat Sealing Foil followed by 30 min agitation at room temperature and analyzed by LC-MS/MS (as described in a following section). The values were normalized by cell count for each well and are reported as the fold change over control (vehicle, DMSO) or nmol/million cells.

2.7. Mouse Sterol Measurements

To 10 μL of mouse serum or tissue lysate, we added 800 μL of Folch solution containing 0.25 mg/mL TPP, 0.005% BHT, and the internal standards d_7-7-DHC (13 ng), $^{13}C_3$-DES (100 ng), $^{13}C_3$-LAN (100 ng), d_7-CHOL (34 ng), followed by the addition of 400 μL of 0.9% NaCl. The resulting mixture was vortexed and centrifuged. The lower organic phase was recovered and dried in SpeedVac. 100 μL of 2 mg/mL freshly prepared PTAD solution in MeOH was added to the residues of the extracts for derivatization as previously described [47].

The solutions were incubated for 30 min at room temperature with constant shaking, transferred into sample vials and placed in an Acquity UPLC system equipped with ANSI-compliant well plate holder coupled to a Thermo Scientific TSQ Quantis mass spectrometer equipped with an APCI source. Then, 10 μL was injected onto the column (Phenomenex Luna Omega C18, 1.6 μm, 100 Å, 2.1 × 100 mm) with 60% MeOH (0.1% v/v acetic acid) 40% acetonitrile (0.1% v/v acetic acid) mobile phase for a 1.4 min runtime at a flow rate of 500 μL/min.

Natural sterols were analyzed by selective reaction monitoring (SRM) using the following transitions: Chol $369 \rightarrow 369$, 7-DHC $560 \rightarrow 365$, desmosterol $592 \rightarrow 560$, and lanosterol $634 \rightarrow 602$, with retention times of 1.5, 0.78, 0.55, 0.76, and 0.61 min, respectively. SRMs for the internal standards were set to: d_7-CHOL $376 \rightarrow 376$, d_7_7-DHC $567 \rightarrow 372$, $^{13}C_3$-DES $595 \rightarrow 563$, and $^{13}C_3$-LAN $637 \rightarrow 605$. Final sterol numbers are reported as nmol/μL of serum or nmol/mg protein.

2.8. Drug Extraction

Drug extraction was performed using our previously published protocol [48,49]. Briefly, to 100 μL of sample, we added 188 μL H_2O, 10 μL internal standard (d_8-aripiprazole) and 75 μL of 4.5 M ammonium hydroxide. The samples were then vortexed vigorously for 1 min. Following vortexing, 950 μL of methyl *tert*-butyl ether (MTBE) was added to each sample followed by another minute of vortexing. Samples were then centrifuged at $10,000 \times g$ for 10 min. The top organic layer was collected to a glass autosampler vial and dried in a SpeedVac. After samples were dried 100 μL of MeOH/$NH_3 \cdot H_2O$ (95:5, v/v) was added to each vial, briefly vortexed and then transferred to a chromatography vial insert for LC-MS/MS analysis.

2.9. Drug Measurements

Metoprolol levels were acquired in an Acquity UPLC system coupled to a Thermo Scientific TSQ Quantis mass spectrometer using an ESI source in the positive ion mode. 10 μL of each sample was injected onto the column (Phenomenex Luna Omega C18, 1.6 μm, 100 Å, 2.1 × 50 mm) using water (0.1% v/v acetic acid) (solvent A) and acetonitrile (0.1% v/v acetic acid) (solvent B) as mobile phase. The gradient was: 10% to 40% B for 0.5 min; 40% to 95% B for 0.4 min; 95% B for 1.5 min; 95% to 10% B for 0.1 min; 10% B for 0.5 min. Metoprolol was analyzed by selective reaction monitoring (SRM) using the following transition: metoprolol $268 \rightarrow 133$. The SRM for the internal standards (d_8-aripiprazole) was set to $456 \rightarrow 293$, and the response factors were determined to accurately determine the drug levels. The final drug levels are reported as ng/mg of protein.

2.10. Statistics

Statistical analyses were performed using GraphPad Prism 9 for Windows. Unpaired two-tailed *t*-tests were performed for individual comparisons between two groups. The

Welch's correction was employed when the variances between the two groups were significantly different. Ordinary one-way ANOVA with Dunnett's multiple comparison correction was employed to compare the difference between each concentration and the control condition. When the Brown–Forsythe test for equal variances returned $p < 0.05$ Brown–Forsythe and Welch ANOVA tests were employed with Dunnett's T3 correction for multiple comparisons. The p values for statistically significant differences are highlighted in the figure legends.

3. Results

3.1. Multiple Beta-Blockers Inhibit Sterol Biosynthesis In Vitro

To investigate the effects of commonly used beta-blockers on sterol biosynthesis, we selected six commonly used beta-blockers that were prescribed > 125 million times/year in the US alone (Figure S2) [50]. The screening for sterol biosynthesis inhibiting properties of atenolol (ATN), carvedilol (CRV), labetalol (LAB), metoprolol (MTP), nebivolol (NEB), and propranolol (PRO) was performed in four distinct in vitro systems: Neuro2a and HepG2 cell lines, primary neurons and astrocytes. We tested the medications at 100 nM, 200 nM, 500 nM, and 1 µM concentrations and compared the outcomes to vehicle-exposed cultures.

Across all four experimental systems we observed a sharp rise in 7-DHC and DES reduction for NEB, MTP, and LAB (Figure 1). This effect was most prominent for all medications in HepG2 cells, while the weakest response was observed in Neuro2a cells. The most potent inhibitor of sterol biosynthesis was NEB (up to 600-fold 7-DHC increase in HepG2 cells), followed by MTP (200-fold 7-DHC increase in HepG2 cells). The observed effects were dose-dependent for NEB, MTP, and LAB, with no significant effects of ATN, CRV and PRO on sterol biosynthesis (Figures S3–S7). Notably, while both NEB and MTP significantly reduced CHOL levels, this reduction was small in comparison to the observed DES reduction. Lanosterol (LAN) levels were not significantly changed in any of our experiments as the LAN synthesizing enzymes are not affected by any of the tested medications.
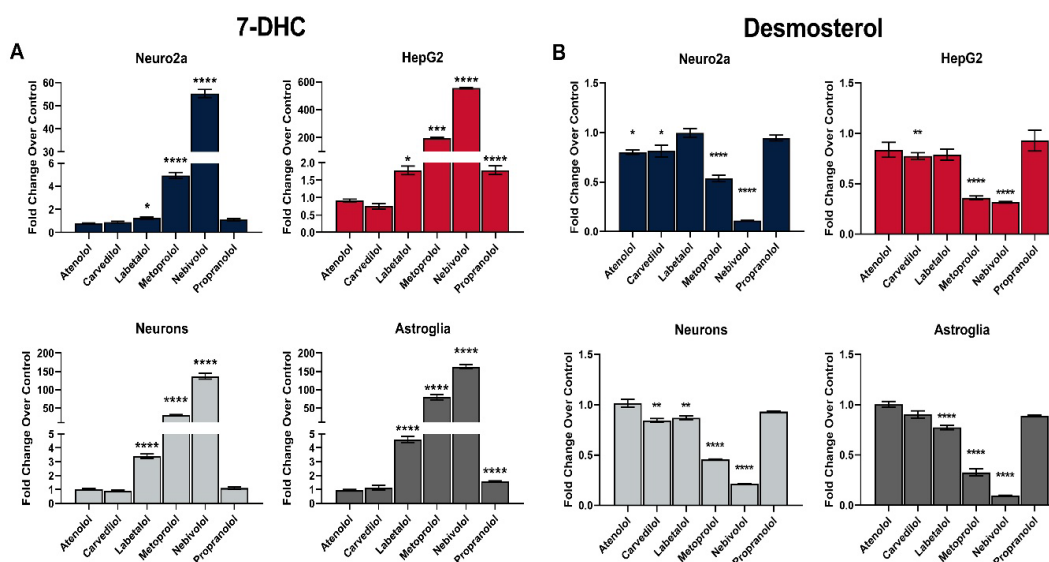

Figure 1. Select β-blockers elevate 7-DHC (**A**) and reduce DES (**B**) levels in vitro. Neuro2a, HepG2, primary neurons and astroglia were treated with 1 µM of six β-blockers or vehicle in cholesterol-free defined media for 48 h (Neuro2a and HepG2) or 6 days (neurons and astroglia). 7-DHC levels were analyzed by LC-MS/MS. The y-axes have different scales for visualization purposes. Note that NEB, MTP, and LAB robustly and significantly increase 7-DHC in all cell types. Values reported as mean ± SEM over vehicle-treated control; statistical significance: * $p < 0.05$; ** $p < 0.01$ *** $p < 0.001$; **** $p < 0.0001$.

3.2. MTP Is a Strong Inhibitor of Sterol Biosynthesis In Vitro

While NEB showed the highest sterol biosynthesis inhibitory effects in our initial screening, based on the sheer volume prescription we decided to focus our follow-up experiments on MTP. MTP is the fifth most commonly utilized medication in the US, with >75 M yearly prescriptions [50]. It is often prescribed to pregnant women [37,39–42,48,51–54]. In the preliminary experiments MTP exposure resulted in a 50–100-fold elevation of 7-DHC in neurons and astrocytes. These increased 7-DHC levels were concerning, as patients with Smith–Lemli–Opitz syndrome (SLOS), due to compound genetic mutations of the DHCR7 gene show a 30–50-fold elevation of 7-DHC in their sera compared to sera of healthy individuals. However, we acknowledge that the magnitude of changes in our in vitro system cannot be directly compared to the 7-DHC elevation seen in SLOS patients.

The dose-dependent effects of MTP on post-lanosterol synthesis are shown in Figures 2 and 3. In comparison to vehicle-treated cultures, the strongest, highly significant increase were observed in 7-DHC levels. The data across the 4 cell lines suggested that the degree of sterol biosynthesis inhibition by MTP is highly dependent on the tissue type: HepG2 cells were approximately 50-fold more affected by MTP than Neuro2a cells (200-fold increase over vehicle-treated baseline vs. five-fold change over baseline for 7-DHC levels; Figure 2).
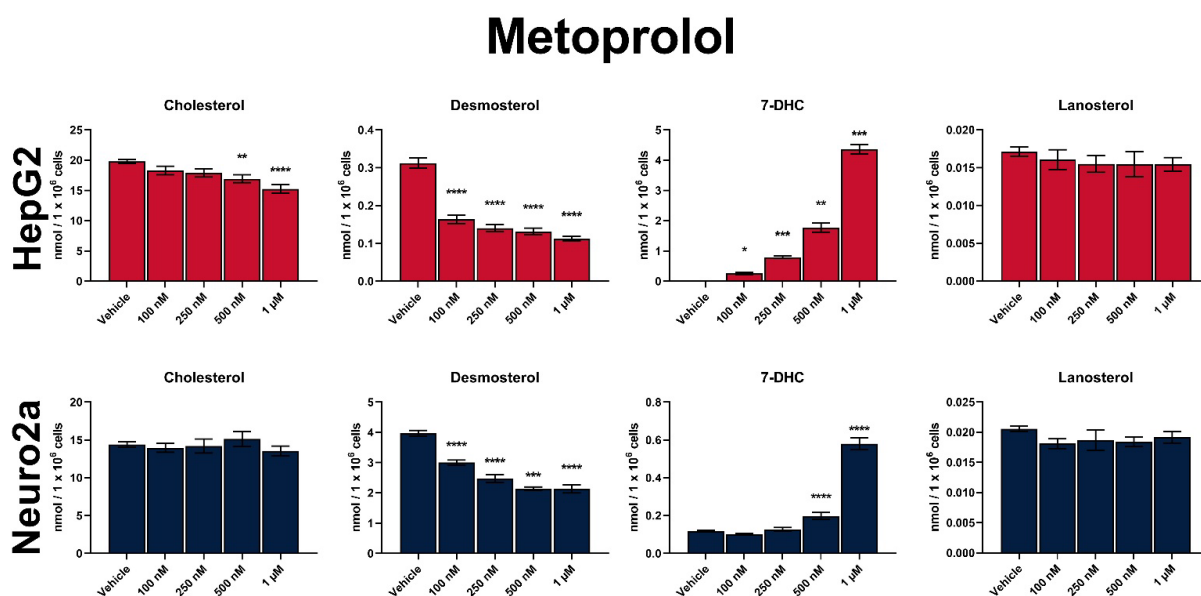

Figure 2. Dose-dependent sterol response of HepG2 and Neuro2a cells treated with MTP. Values reported as nmol/million cells. Statistical significance: * $p < 0.05$; ** $p < 0.01$; *** $p < 0.001$; **** $p < 0.0001$ vs. vehicle treatment.

Due to the apparent DHCR7 inhibition by MTP both the Kandutsch–Russel and Bloch branches of the sterol biosynthesis were affected (Figure S1), and we also observed a strong and significant decrease in DES. Residual DES levels decreased to approximately 45% of those seen in vehicle-treated HepG2 cultures, with the smallest effects observed in Neuro2a cells (70% of sham-treated cultures). CHOL levels seemed to be mostly resilient to MTP treatment across all cell lines (except the highest concentration in HepG2 cells), which is likely due to the short treatment window, residual CHOL level in the cultures, and slow CHOL turnover.
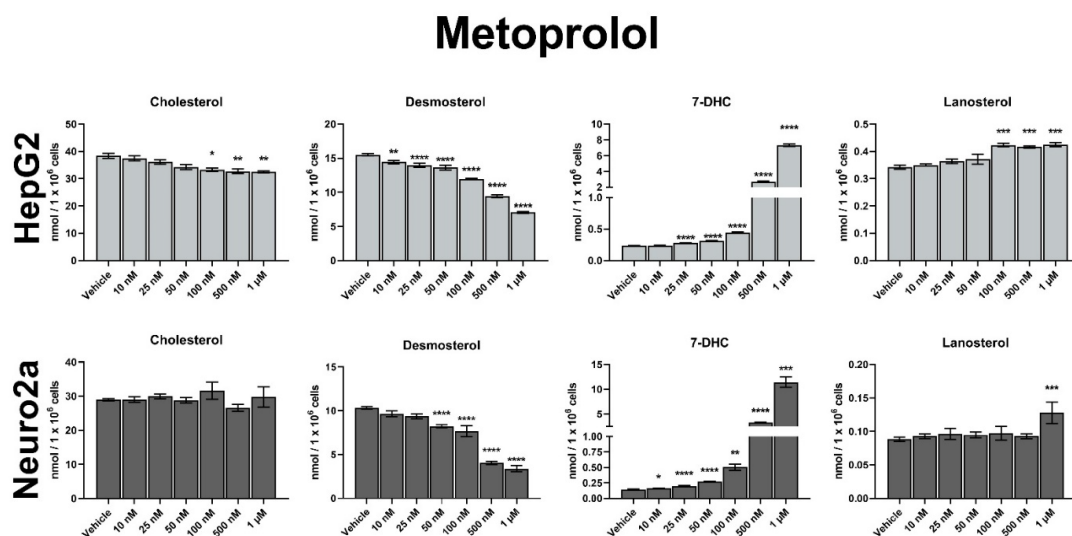
Metoprolol

Figure 3. Dose-dependent sterol response of neurons and astrocytes treated with MTP. Values reported as nmol/million cells. Note the broken *y*-axis for 7-DHC. Statistical significance: * $p < 0.05$; ** $p < 0.01$; *** $p < 0.001$; **** $p < 0.0001$ vs. vehicle treatment.

3.3. MTP Inhibits Sterol Biosynthesis in Maternal Mouse Tissues

Due to the well-documented biological effects of 7-DHC on development, obtained in vitro data, and the use of MTP by pregnant women, we decided to test the MTP effects in a maternal exposure model in mice. Pregnant mice were injected daily with 35 mg/kg MTP or vehicle from embryonic day 12–19 (E12–E19). This dose was selected to mimic the dosage typically prescribed to human patients.

At E19, the pregnant dams were killed, and the maternal brain, heart, kidney, liver, sciatic nerve, and serum were harvested for sterol profiling. Maternal brain regions were further dissected, and the neocortex, hippocampus, striatum, midbrain, cerebellum, and medulla/pons were also analyzed using LC-MS/MS. The analysis of brain regions revealed that all six investigated maternal brain regions had significantly elevated 7-DHC levels (Figure 4). In addition, we also observed a relatively uniform, significant 7-DHC elevation in the heart, kidney, sciatic nerve, and serum of the same pregnant dams (Figure S8). Presumably due the low turnover rate of CHOL and short treatment window, we did not observe significant changes in CHOL levels in any of the investigated tissues (Figure S9).

3.4. Maternal Exposure to MTP Alters the Sterol Composition in the Tissue of Offspring

Next, we assessed if maternal MTP can cross the placenta and impact embryonic brain sterols biosynthesis. Maternal exposure to MTP resulted in a strong and highly significant, >10-fold elevation of 7-DHC in the offspring brain ($p < 0.0001$) (Figure 5). In contrast, DES levels decreased by approximately 15% ($p < 0.001$), with non-significant effects on CHOL and LAN. As a result, 7-DHC/CHOL ratio showed an approximately nine-fold increase ($p < 0.0001$). We did not observe any differences in the sterol profile between male and female pups in response to the maternal MTP treatment.

Following the assessment of the brain, we performed a similar assessment of post-lanosterol sterol biosynthesis on the heart (Figure 6) and liver (Figure 7) of offspring that were maternally exposed to MTP. The overall results in both peripheral tissues were comparable to those that seen in the brain, suggesting that MTP action is consistent on the peripheral and central sterol biosynthesis. Notably, absolute analyte levels were different across the three investigated tissues, with the CNS pool showing the highest absolute sterol levels at baseline (CHOL: Brain—181 nM/mg protein; Heart—73 nM/mg protein; Liver—70 nM/mg protein).
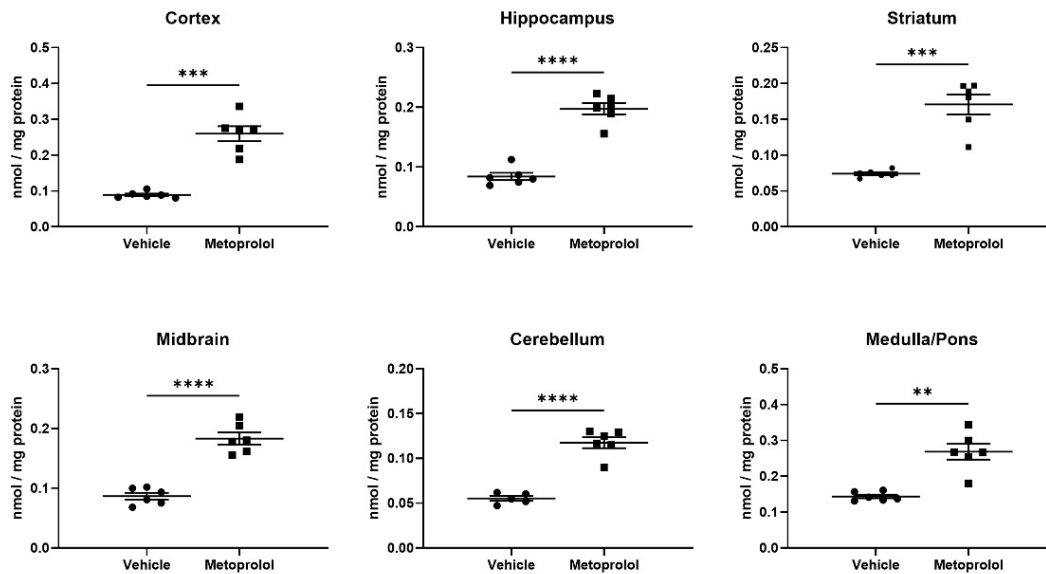
7-DHC by Maternal Brain Region

Figure 4. Metoprolol elevates 7-DHC throughout the maternal brain. Pregnant mice were treated with 35 mg/kg MTP from E12 to E19. Dam brains were analyzed for sterol content by LC-MS/MS. Statistical significance: ** $p < 0.01$; *** $p < 0.001$; **** $p < 0.0001$ vs. vehicle treatment. Note that 7-DHC baseline levels in the vehicle-treated animals are different across the brain regions, and that a robust 7-DHC elevation is evident in all investigated brain regions. In the same brain regions, cholesterol levels were unchanged (Figure S9).
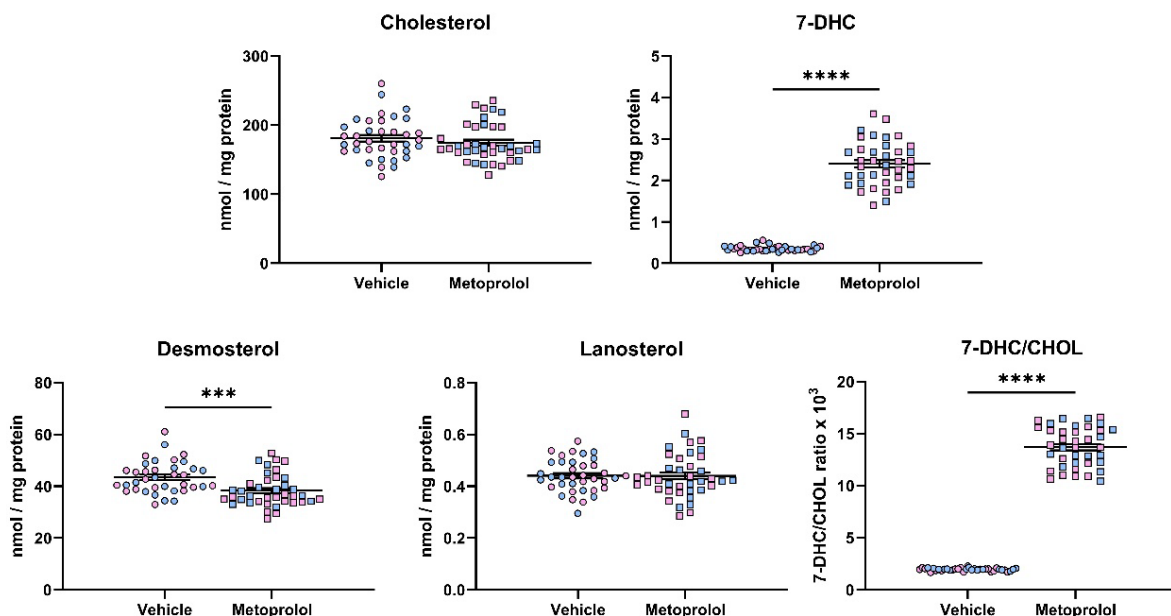
Offspring Brain

Figure 5. Maternal exposure to metoprolol results in strong elevation of 7-DHC and decreased desmosterol levels in the offspring brain. Pregnant mice were treated with 35 mg/kg MTP from E12 to E19. E19 brains were analyzed for sterol content by LC-MS/MS. Each symbol represents a sample originating from a single offspring brain. Blue fill = male embryos, pink fill = female embryos. Note the strong change in 7-DHC/CHOL (precursor/product) ratio. Statistical significance: *** $p < 0.001$; **** $p < 0.0001$.
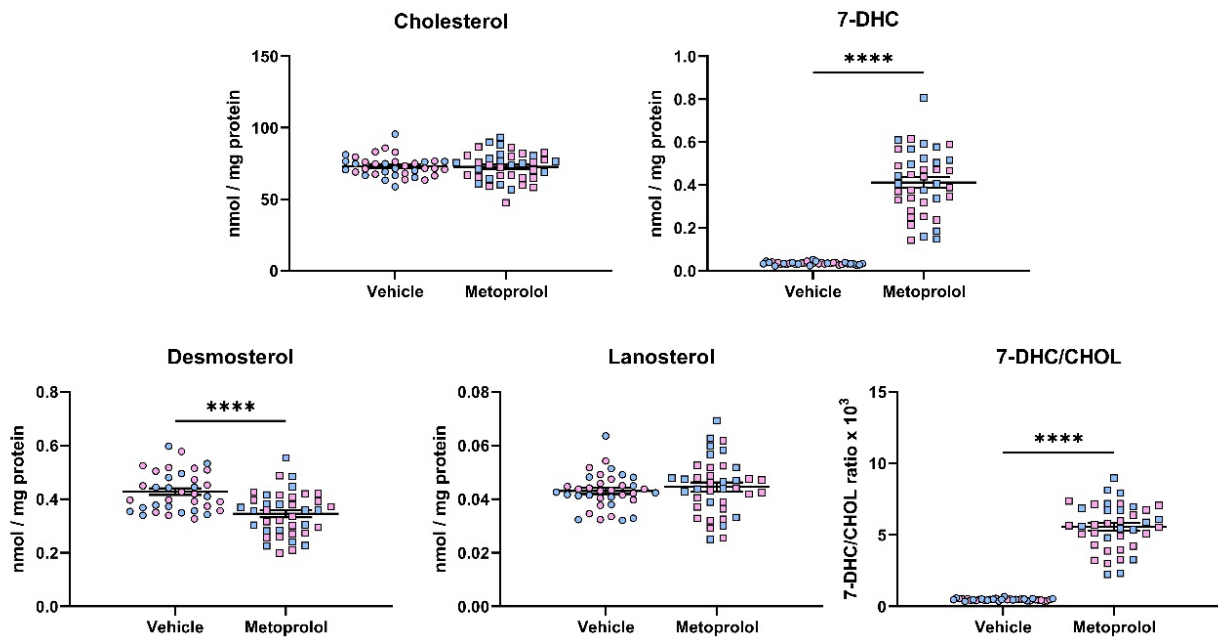
Offspring Heart

Figure 6. Maternal exposure to metoprolol results in strong elevation of 7-DHC and decreased desmosterol levels in the offspring heart. Pregnant mice were treated with 35 mg/kg MTP from E12 to E19. E19 hearts were analyzed for sterol content by LC-MS/MS. Each symbol represents a sample originating from a single offspring heart. Blue fill = male embryos, pink fill = female embryos. Note the strong change in 7-DHC/CHOL (precursor/product) ratio. Statistical significance: **** $p < 0.0001$.
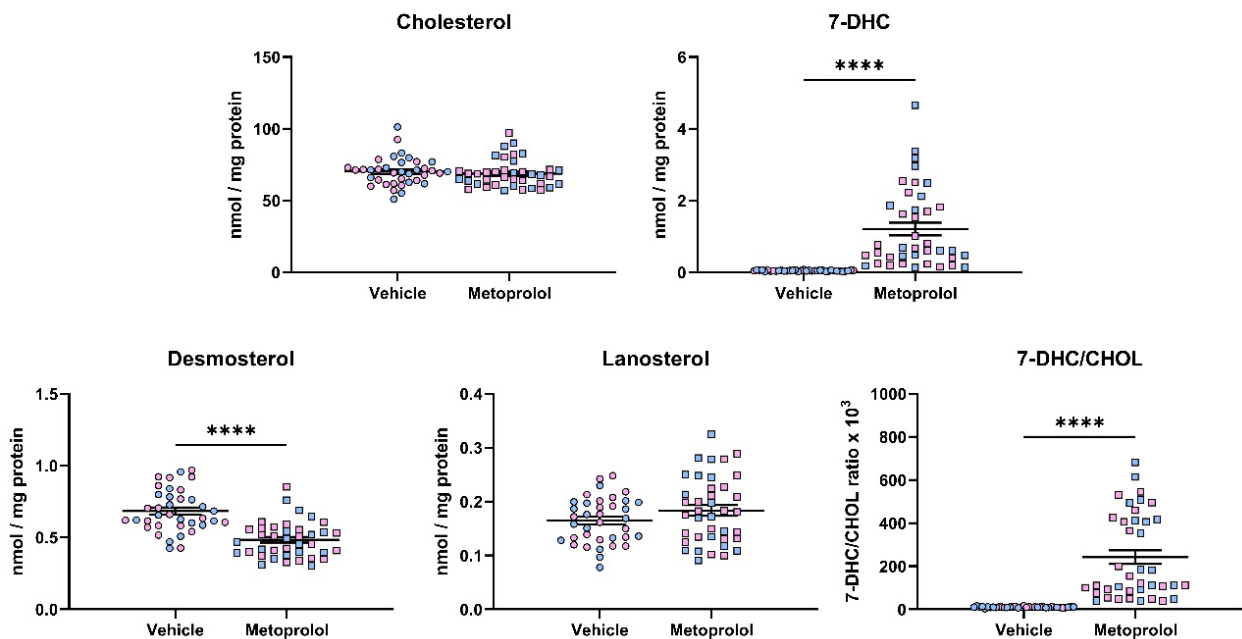
Offspring Liver

Figure 7. Maternal exposure to metoprolol results in strong elevation of 7-DHC and decreased desmosterol levels in the offspring liver. Pregnant mice were treated with 35 mg/kg MTP from E12 to E19. E19 livers were analyzed for sterol content by LC-MS/MS. Each symbol represents a sample originating from a single offspring liver. Blue fill = male embryos, pink fill = female embryos. Note the strong change in 7-DHC/CHOL (precursor/product) ratio. Statistical significance: **** $p < 0.0001$.

These results suggest that MTP is a strong developmental inhibitor of sterol biosynthesis across both the CNS and peripheral tissues, primally interfering with the function of the DHCR7 enzyme. Notably, no statistically significant sex differences were observed.

3.5. Correlation of MTP Levels with Sterol Precursors

Finally, we examined the correlation between DES and 7-DHC levels with MTP levels in the offspring brain and liver (Figure 8). DES levels were not correlated with the observed MTP levels in the exposed offspring brain or liver, while a complex correlation pattern emerged for the 7-DHC/MTP levels. In the brain, 7-DHC showed a significant, negative correlation with MTP levels ($R^2 = 0.32$, $p = 0.0001$), while in the liver 7-DHC showed a strong, positive correlation with MTP ($R^2 = 0.78$, $p < 0.0001$).
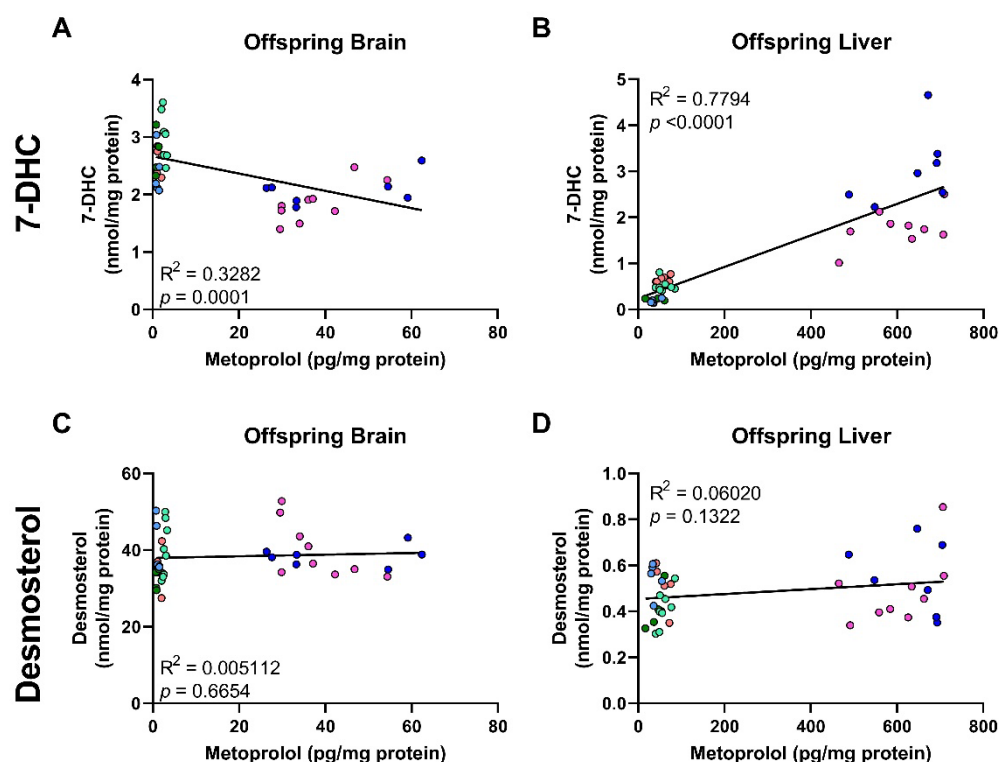

Figure 8. Metoprolol levels are correlated with 7-DHC levels (**A**,**B**) and DES levels (**C**,**D**) in the tissues of maternally exposed offspring. Only results obtained from MTP-exposed offspring are plotted. Each symbol corresponds to a single offspring sample, and samples from littermates are denoted by the same color. Lines denote simple linear regression. Note the variability between litters, but consistency within littermates.

We attribute this to the very short half-life of MTP in the brain, and a delay between maximum brain concentration of MTP and peak 7-DHC concentration. We propose that while MTP levels are the highest in the brain, the 7-DHC levels are still rising, and by the time 7-DHC levels peak MTP is already cleared from the brain tissue. Apparently, this fast turnover of MTP is not present in the liver of the same maternally exposed offspring, as the 7-DHC and MTP levels are almost perfectly correlated.

4. Discussion

The six beta-blockers we tested accounted for over 125 million prescriptions in 2019 in the US alone [55]. While beta-blockers are generally well-tolerated and are known to be safe and life-saving drugs, they have also been known to cause CNS side effects in a subset of patients [56–64]. These side effects include but are not limited to psychiatric conditions, such as bizarre and vivid dreams, sleep disturbances, delirium, psychosis and

visual hallucinations [60,64]. These CNS effects have been primarily correlated with the lipophilicity of the beta-blocker, which allows for rapid penetration of the blood-brain barrier [64–67].

Furthermore, recent studies have revealed that chronic administration of MTP induced markers of phagocytosis in the brain and impaired cognitive behavior in both wild-type and amyloid-beta protein precursor model of Alzheimer's disease in mice [68].

On the other hand, hydrophilic beta-blockers, such as atenolol have been shown to induce signaling molecules, such as NO and H_2O_2 in the hypothalamus without crossing the BBB [69]. Hydrogen peroxide can contribute to oxidative stress [70], which can also affect sterol biosynthesis [17,71] and cell viability through the formation of oxysterols [18–20]. Additionally, oxysterols have been shown to play a role in CNS autoimmune processes [72]. This suggests that, while hydrophilic beta-blockers may not cross the BBB, they still may affect CNS development and function.

CNS-specific side effects of beta-blockers have been assumed to be a result of adrenergic receptor-mediated mechanisms [73]. However, in light of our findings, we believe that the explanation is more complex. We propose that MTP side effects arise as a complex interplay between beta-adrenergic effects [62,74] and sterol biosynthesis disruptions [75]. Thus, deciphering the root cause of the observed side effects stands as a difficult task, further complicated by seemingly multiple mechanisms of action occurring simultaneously [76,77]. This remains an interesting avenue for future studies, particularly when considering the large number of beta-blocker prescriptions currently being given.

Our studies show that the developing brain is extremely susceptible to the sterol biosynthesis inhibiting effects of MTP, and perhaps other commonly used beta-blockers, such as nebivolol. Worryingly, beta-blockers are the most prescribed cardiac medications for pregnant women [78]. Furthermore, psychotropic medications with sterol biosynthesis side effects (aripiprazole, trazodone, haloperidol, and cariprazine) [1,48] are also commonly prescribed during pregnancy, often by different providers.

This raises the possibility that the sterol biosynthesis inhibiting effects of these two classes of medications will summate, further elevating the 7-DHC levels to dangerous levels in the developing brain. This view is supported by a recent study showing that long-term exposure to MTP as a part of polypharmacy (concurrent use of five or more drugs) lead to a deficit in cognitive function in young adult female mice [79].

The potential interactions between beta-blockers and psychotropic medications are also important to consider in adult patients, not only during pregnancy. There is a high level of comorbidity between cardiovascular diseases which may call for beta-blockers and bipolar disorder or schizophrenia [80]. In fact, beta-blockers accounted for 25% of all cases that had interactions with antipsychotic medications [80]. Unfortunately, while it is considered a questionable practice, beta-blockers are often prescribed alongside standard antipsychotic treatments to treat cardiovascular disease and extrapyramidal symptoms, such as akathisia [81–83].

One should also consider the potential for interactions as a result of sterol-inhibiting polypharmacy, as it appears that there are multiple chemical substructures that inhibit DHCR7. We previously identified 2,3-dichlorophenylpiperazine (2,3-DCPP) as being capable of inhibiting DHCR7 [84]. However, unlike aripiprazole and cariprazine, two DHCR7 inhibitors sharing the 2,3-DCPP motif [30,31,45,48,84–87] the beta-blockers discussed in the present study contain no such common moieties (Figure S10), suggesting that there are multiple chemical substructures that may inhibit DHCR7 and elevate 7-DHC.

The public health implications of our findings are noteworthy. As obesity is one of the leading risk factors for high blood pressure and other cardiovascular disease [88–93], the ongoing obesity pandemic [92,94,95] would suggest that MTP prescriptions will continue to increase. This will likely extend to pregnant women as well, as MTP is not currently contraindicated for pregnancy. Thus, it is likely that prescription of MTP (and other beta-blockers) will continue to increase in pregnant women to control blood pressure due to

obesity, thereby, exposing more fetuses to a potentially harmful increase in 7-DHC during critical developmental periods.

This may be further compounded in the 1–3% of the human population that carry single-allele DHCR7 mutations who already have increased baseline 7-DHC levels [13,96,97] where the potential for a drug × gene interaction could lead to even worse outcomes. In summary, based on the documented teratogenicity of DCHR7 inhibitors [22], the DHCR7 inhibitory side effects of MTP are a cause for caution, particularly in the context of pregnancy, polypharmacy and DHCR7 genetic liability.

Supplementary Materials: The following supporting information can be downloaded at: https://www.mdpi.com/article/10.3390/biom12091211/s1, Figure S1: Post-lanosterol cholesterol biosynthesis pathway; Figure S2. Prescription data, action and CNS-related side effects of investigated beta-blockers; Figure S3: Dose-dependent sterol response of HepG2 and Neuro2a cells treated with atenolol; Figure S4: Dose-dependent sterol response of HepG2 and Neuro2a cells treated with carvedilol; Figure S5: Dose-dependent sterol response of HepG2 and Neuro2a cells treated with labetalol; Figure S6: Dose-dependent sterol response of HepG2 and Neuro2a cells treated with nebivolol; Figure S7: Dose-dependent sterol response of HepG2 and Neuro2a cells treated with propranolol; Figure S8: Short-term MTP treatment elevates 7-DHC levels in the peripheral tissues of pregnant mouse dams; Figure S9: Short-term MTP treatment has no significant effect on cholesterol levels in the brain of pregnant mouse dams. Figure S10: Chemical structure of beta-blockers and known DHCR7 inhibitors.

Author Contributions: Conceptualization, L.B.A. and K.M.; funding acquisition, K.M.; investigation, L.B.A.; project administration, K.M.; resources, K.M.; supervision, K.M.; validation, K.M.; visualization, L.B.A.; writing, L.B.A. and K.M. All authors have read and agreed to the published version of the manuscript.

Institutional Review Board Statement: The use of mice in this study was approved by the Institutional Animal Care and Use Committee of UNMC Protocol # 21-011-03-FC (approved 3 November 2021).

Data Availability Statement: Not applicable.

Conflicts of Interest: The authors declare no conflict of interest.

References

1. Korade, Z.; Heffer, M.; Mirnics, K. Medication effects on developmental sterol biosynthesis. *Mol. Psychiatry* **2022**, *27*, 490–501. [CrossRef] [PubMed]
2. Dietschy, J.M. Central nervous system: Cholesterol turnover, brain development and neurodegeneration. *Biol. Chem.* **2009**, *390*, 287–293. [CrossRef] [PubMed]
3. Dietschy, J.M.; Turley, S.D. Cholesterol metabolism in the brain. *Curr. Opin. Lipidol.* **2001**, *12*, 105–112. [CrossRef] [PubMed]
4. Dietschy, J.M.; Turley, S.D. Thematic review series: Brain Lipids. Cholesterol metabolism in the central nervous system during early development and in the mature animal. *J. Lipid Res.* **2004**, *45*, 1375–1397. [CrossRef] [PubMed]
5. Nes, W.D. Biosynthesis of cholesterol and other sterols. *Chem. Rev.* **2011**, *111*, 6423–6451. [CrossRef]
6. Tint, G.S.; Yu, H.; Shang, Q.; Xu, G.; Patel, S.B. The use of the Dhcr7 knockout mouse to accurately determine the origin of fetal sterols. *J. Lipid Res.* **2006**, *47*, 1535–1541. [CrossRef]
7. Pfrieger, F.W. Role of cholesterol in synapse formation and function. *Biochim. Biophys. Acta* **2003**, *1610*, 271–280. [CrossRef]
8. Shrivastava, S.; Paila, Y.D.; Kombrabail, M.; Krishnamoorthy, G.; Chattopadhyay, A. Role of Cholesterol and Its Immediate Biosynthetic Precursors in Membrane Dynamics and Heterogeneity: Implications for Health and Disease. *J. Phys. Chem. B* **2020**, *124*, 6312–6320. [CrossRef]
9. Korade, Z.; Kenworthy, A.K. Lipid rafts, cholesterol, and the brain. *Neuropharmacology* **2008**, *55*, 1265–1273. [CrossRef]
10. Fitzky, B.U.; Witsch-Baumgartner, M.; Erdel, M.; Lee, J.N.; Paik, Y.K.; Glossmann, H.; Utermann, G.; Moebius, F.F. Mutations in the Delta7-sterol reductase gene in patients with the Smith-Lemli-Opitz syndrome. *Proc. Natl. Acad. Sci. USA* **1998**, *95*, 8181–8186. [CrossRef]

11. Lamberson, C.R.; Muchalski, H.; McDuffee, K.B.; Tallman, K.A.; Xu, L.; Porter, N.A. Propagation rate constants for the peroxidation of sterols on the biosynthetic pathway to cholesterol. *Chem. Phys. Lipids* **2017**, *207*, 51–58. [CrossRef] [PubMed]

12. Porter, F.D. RSH/Smith-Lemli-Opitz syndrome: A multiple congenital anomaly/mental retardation syndrome due to an inborn error of cholesterol biosynthesis. *Mol. Genet. Metab.* **2000**, *71*, 163–174. [CrossRef] [PubMed]

13. Porter, F.D. Smith-Lemli-Opitz syndrome: Pathogenesis, diagnosis and management. *Eur. J. Hum. Genet.* **2008**, *16*, 535–541. [CrossRef] [PubMed]

14. Porter, F.D.; Herman, G.E. Malformation syndromes caused by disorders of cholesterol synthesis. *J. Lipid Res.* **2011**, *52*, 6–34. [CrossRef] [PubMed]

15. Xu, L.; Davis, T.A.; Porter, N.A. Rate constants for peroxidation of polyunsaturated fatty acids and sterols in solution and in liposomes. *J. Am. Chem. Soc.* **2009**, *131*, 13037–13044. [CrossRef]

16. Xu, L.; Korade, Z.; Porter, N.A. Oxysterols from free radical chain oxidation of 7-dehydrocholesterol: Product and mechanistic studies. *J. Am. Chem. Soc.* **2010**, *132*, 2222–2232. [CrossRef]

17. Xu, L.; Korade, Z.; Rosado, D.A., Jr.; Mirnics, K.; Porter, N.A. Metabolism of oxysterols derived from nonenzymatic oxidation of 7-dehydrocholesterol in cells. *J. Lipid Res.* **2013**, *54*, 1135–1143. [CrossRef]

18. Pfeffer, B.A.; Xu, L.; Porter, N.A.; Rao, S.R.; Fliesler, S.J. Differential cytotoxic effects of 7-dehydrocholesterol-derived oxysterols on cultured retina-derived cells: Dependence on sterol structure, cell type, and density. *Exp. Eye Res.* **2016**, *145*, 297–316. [CrossRef]

19. Xu, L.; Mirnics, K.; Bowman, A.B.; Liu, W.; Da, J.; Porter, N.A.; Korade, Z. DHCEO accumulation is a critical mediator of pathophysiology in a Smith-Lemli-Opitz syndrome model. *Neurobiol. Dis.* **2012**, *45*, 923–929. [CrossRef]

20. Korade, Z.; Xu, L.; Shelton, R.; Porter, N.A. Biological activities of 7-dehydrocholesterol-derived oxysterols: Implications for Smith-Lemli-Opitz syndrome. *J. Lipid Res.* **2010**, *51*, 3259–3269. [CrossRef]

21. Xiao, J.; Li, W.; Zheng, X.; Qi, L.; Wang, H.; Zhang, C.; Wan, X.; Zheng, Y.; Zhong, R.; Zhou, X.; et al. Targeting 7-Dehydrocholesterol Reductase Integrates Cholesterol Metabolism and IRF3 Activation to Eliminate Infection. *Immunity* **2020**, *52*, 109–122.e106. [CrossRef] [PubMed]

22. Boland, M.R.; Tatonetti, N.P. Investigation of 7-dehydrocholesterol reductase pathway to elucidate off-target prenatal effects of pharmaceuticals: A systematic review. *Pharmacogenomics J.* **2016**, *16*, 411–429. [CrossRef] [PubMed]

23. DeBarber, A.E.; Eroglu, Y.; Merkens, L.S.; Pappu, A.S.; Steiner, R.D. Smith-Lemli-Opitz syndrome. *Expert Rev. Mol. Med.* **2011**, *13*, e24. [CrossRef]

24. Kelley, R.I.; Hennekam, R.C. The Smith-Lemli-Opitz syndrome. *J. Med. Genet.* **2000**, *37*, 321–335. [CrossRef]

25. Smith, D.W.; Lemli, L.; Opitz, J.M. A Newly Recognized Syndrome of Multiple Congenital Anomalies. *J. Pediatr.* **1964**, *64*, 210–217. [CrossRef]

26. Kadoguchi, M.; Arakawa, H.; Honda, R.; Hotta, K.; Shirasaka, Y.; Deguchi, Y.; Tamai, I. Characterization of Aripiprazole Uptake Transporter in the Blood-Brain Barrier Model hCMEC/D3 Cells by Targeted siRNA Screening. *Pharm. Res.* **2022**, *39*, 1549–1559. [CrossRef] [PubMed]

27. Toth, M.; Varrone, A.; Steiger, C.; Laszlovszky, I.; Horvath, A.; Kiss, B.; Gyertyan, I.; Adham, N.; Halldin, C.; Gulyas, B. Brain uptake and distribution of the dopamine D3/D2 receptor partial agonist [11 C]cariprazine: An in vivo positron emission tomography study in nonhuman primates. *Synapse* **2013**, *67*, 258–264. [CrossRef]

28. Banks, W.A. Characteristics of compounds that cross the blood-brain barrier. *BMC Neurol.* **2009**, *9* (Suppl. 1), S3. [CrossRef]

29. Saija, A.; Princi, P.; Imperatore, C.; De Pasquale, R.; Costa, G. Ageing influences haloperidol-induced changes in the permeability of the blood-brain barrier in the rat. *J. Pharm. Pharmacol.* **1992**, *44*, 450–452. [CrossRef]

30. Genaro-Mattos, T.C.; Allen, L.B.; Anderson, A.; Tallman, K.A.; Porter, N.A.; Korade, Z.; Mirnics, K. Maternal aripiprazole exposure interacts with 7-dehydrocholesterol reductase mutations and alters embryonic neurodevelopment. *Mol. Psychiatry* **2019**, *24*, 491–500. [CrossRef]

31. Genaro-Mattos, T.C.; Anderson, A.; Allen, L.B.; Tallman, K.A.; Porter, N.A.; Korade, Z.; Mirnics, K. Maternal cariprazine exposure inhibits embryonic and postnatal brain cholesterol biosynthesis. *Mol. Psychiatry* **2020**, *25*, 2685–2694. [CrossRef]

32. Korade, Z.; Allen, L.B.; Anderson, A.; Tallman, K.A.; Genaro-Mattos, T.C.; Porter, N.A.; Mirnics, K. Trazodone effects on developing brain. *Transl. Psychiatry* **2021**, *11*, 85. [CrossRef] [PubMed]

33. Korade, Z.; Liu, W.; Warren, E.B.; Armstrong, K.; Porter, N.A.; Konradi, C. Effect of psychotropic drug treatment on sterol metabolism. *Schizophr. Res.* **2017**, *187*, 74–81. [CrossRef] [PubMed]

34. Wages, P.A.; Kim, H.H.; Korade, Z.; Porter, N.A. Identification and characterization of prescription drugs that change levels of 7-dehydrocholesterol and desmosterol. *J. Lipid Res.* **2018**, *59*, 1916–1926. [CrossRef] [PubMed]

35. Kim, H.Y.; Korade, Z.; Tallman, K.A.; Liu, W.; Weaver, C.D.; Mirnics, K.; Porter, N.A. Inhibitors of 7-Dehydrocholesterol Reductase: Screening of a Collection of Pharmacologically Active Compounds in Neuro2a Cells. *Chem. Res. Toxicol.* **2016**, *29*, 892–900. [CrossRef]

36. Korade, Z.; Kim, H.Y.; Tallman, K.A.; Liu, W.; Koczok, K.; Balogh, I.; Xu, L.; Mirnics, K.; Porter, N.A. The Effect of Small Molecules on Sterol Homeostasis: Measuring 7-Dehydrocholesterol in Dhcr7-Deficient Neuro2a Cells and Human Fibroblasts. *J. Med. Chem.* **2016**, *59*, 1102–1115. [CrossRef]

37. Podymow, T.; August, P. Update on the use of antihypertensive drugs in pregnancy. *Hypertension* **2008**, *51*, 960–969. [CrossRef]

38. Bateman, B.T.; Huybrechts, K.F.; Fischer, M.A.; Seely, E.W.; Ecker, J.L.; Oberg, A.S.; Franklin, J.M.; Mogun, H.; Hernandez-Diaz, S. Chronic hypertension in pregnancy and the risk of congenital malformations: A cohort study. *Am. J. Obstet. Gynecol.* **2015**, *212*, 337.e1–337.e14. [CrossRef]

39. Bateman, B.T.; Heide-Jorgensen, U.; Einarsdottir, K.; Engeland, A.; Furu, K.; Gissler, M.; Hernandez-Diaz, S.; Kieler, H.; Lahesmaa-Korpinen, A.M.; Mogun, H.; et al. beta-Blocker Use in Pregnancy and the Risk for Congenital Malformations: An International Cohort Study. *Ann. Intern. Med.* **2018**, *169*, 665–673. [CrossRef]

40. Podymow, T.; August, P. Antihypertensive drugs in pregnancy. *Semin. Nephrol.* **2011**, *31*, 70–85. [CrossRef]

41. Kayser, A.; Beck, E.; Hoeltzenbein, M.; Zinke, S.; Meister, R.; Weber-Schoendorfer, C.; Schaefer, C. Neonatal effects of intrauterine metoprolol/bisoprolol exposure during the second and third trimester: A cohort study with two comparison groups. *J. Hypertens.* **2020**, *38*, 354–361. [CrossRef] [PubMed]

42. Welzel, T.; Donner, B.; van den Anker, J.N. Intrauterine Growth Retardation in Pregnant Women with Long QT Syndrome Treated with Beta-Receptor Blockers. *Neonatology* **2021**, *118*, 406–415. [CrossRef] [PubMed]

43. Orbach, H.; Matok, I.; Gorodischer, R.; Sheiner, E.; Daniel, S.; Wiznitzer, A.; Koren, G.; Levy, A. Hypertension and antihypertensive drugs in pregnancy and perinatal outcomes. *Am. J. Obstet. Gynecol.* **2013**, *208*, 301.e1–301.e6. [CrossRef] [PubMed]

44. Genaro-Mattos, T.C.; Anderson, A.; Allen, L.B.; Korade, Z.; Mirnics, K. Cholesterol Biosynthesis and Uptake in Developing Neurons. *ACS Chem. Neurosci.* **2019**, *10*, 3671–3681. [CrossRef]

45. Tallman, K.A.; Allen, L.B.; Klingelsmith, K.; Anderson, A.; Genaro-Mattos, T.C.; Mirnics, K.; Porter, N.A.; Korade, Z. Prescription Medications Alter Neuronal and Glial Cholesterol Synthesis. *ACS Chem. Neurosci.* **2021**. [CrossRef]

46. Goudriaan, A.; Camargo, N.; Carney, K.E.; Oliet, S.H.; Smit, A.B.; Verheijen, M.H. Novel cell separation method for molecular analysis of neuron-astrocyte co-cultures. *Front. Cell. Neurosci.* **2014**, *8*, 12. [CrossRef]

47. Liu, W.; Xu, L.; Lamberson, C.; Haas, D.; Korade, Z.; Porter, N.A. A highly sensitive method for analysis of 7-dehydrocholesterol for the study of Smith-Lemli-Opitz syndrome. *J. Lipid Res.* **2014**, *55*, 329–337. [CrossRef]

48. Genaro-Mattos, T.C.; Klingelsmith, K.B.; Allen, L.B.; Anderson, A.; Tallman, K.A.; Porter, N.A.; Korade, Z.; Mirnics, K. Sterol Biosynthesis Inhibition in Pregnant Women Taking Prescription Medications. *ACS Pharmacol. Transl. Sci.* **2021**, *4*, 848–857. [CrossRef]

49. Allen, L.B.; Genaro-Mattos, T.C.; Anderson, A.; Porter, N.A.; Mirnics, K.; Korade, Z. Amiodarone Alters Cholesterol Biosynthesis through Tissue-Dependent Inhibition of Emopamil Binding Protein and Dehydrocholesterol Reductase 24. *ACS Chem. Neurosci.* **2020**, *11*, 1413–1423. [CrossRef]

50. Kane, S.P. Evidence-Based Clinical Decision Support Tools and Calculators for Medical Professionals. Available online: Clincalc.com (accessed on 19 July 2022).

51. Bateman, B.T.; Huybrechts, K.F.; Hernandez-Diaz, S.; Kieler, H.; Zoega, H. beta-Blocker Use in Pregnancy and the Risk for Congenital Malformations. *Ann. Intern. Med.* **2019**, *170*, 909–910. [CrossRef]

52. Hogstedt, S.; Lindberg, B.; Rane, A. Increased oral clearance of metoprolol in pregnancy. *Eur. J. Clin. Pharmacol.* **1983**, *24*, 217–220. [CrossRef] [PubMed]

53. Meidahl Petersen, K.; Jimenez-Solem, E.; Andersen, J.T.; Petersen, M.; Brodbaek, K.; Kober, L.; Torp-Pedersen, C.; Poulsen, H.E. beta-Blocker treatment during pregnancy and adverse pregnancy outcomes: A nationwide population-based cohort study. *BMJ Open* **2012**, *2*. [CrossRef] [PubMed]

54. Ryu, R.J.; Eyal, S.; Easterling, T.R.; Caritis, S.N.; Venkataraman, R.; Hankins, G.; Rytting, E.; Thummel, K.; Kelly, E.J.; Risler, L.; et al. Pharmacokinetics of metoprolol during pregnancy and lactation. *J. Clin. Pharmacol.* **2016**, *56*, 581–589. [CrossRef] [PubMed]

55. ClinCalc. Available online: https://clincalc.com/DrugStats/Drugs/Metoprolol (accessed on 21 July 2022).

56. Burkauskas, J.; Noreikaite, A.; Bunevicius, A.; Brozaitiene, J.; Neverauskas, J.; Mickuviene, N.; Bunevicius, R. Beta-1-Selective Beta-Blockers and Cognitive Functions in Patients With Coronary Artery Disease: A Cross-Sectional Study. *J. Neuropsychiatry Clin. Neurosci.* **2016**, *28*, 143–146. [CrossRef]

57. Burris, J.F. Central nervous system side effects with beta-blockers. *Arch. Intern. Med.* **1988**, *148*, 980. [CrossRef]

58. Cove-Smith, J.R.; Kirk, C.A. CNS-related side-effects with metoprolol and atenolol. *Eur. J. Clin. Pharmacol.* **1985**, *28*, 69–72. [CrossRef]

59. Gliebus, G.; Lippa, C.F. The influence of beta-blockers on delayed memory function in people with cognitive impairment. *Am. J. Alzheimers Dis. Other Demen.* **2007**, *22*, 57–61. [CrossRef]

60. Goldner, J.A. Metoprolol-induced visual hallucinations: A case series. *J. Med. Case Rep.* **2012**, *6*, 65. [CrossRef]

61. Liu, X.; Lou, X.; Cheng, X.; Meng, Y. Impact of metoprolol treatment on mental status of chronic heart failure patients with neuropsychiatric disorders. *Drug Des. Devel. Ther.* **2017**, *11*, 305–312. [CrossRef]

62. McAinsh, J.; Cruickshank, J.M. Beta-blockers and central nervous system side effects. *Pharmacol. Ther.* **1990**, *46*, 163–197. [CrossRef]

63. Rietveld, L.; van der Hoek, T.; van Beek, M.H.; Schellekens, A.F. Familial liability for metoprolol-induced psychosis. *Gen. Hosp. Psychiatry* **2015**, *37*, e625–e626. [CrossRef] [PubMed]

64. Sirois, F.J. Visual hallucinations and metoprolol. *Psychosomatics* **2006**, *47*, 537–538. [CrossRef] [PubMed]

65. Ahmed, A.I.; van Mierlo, P.J.; van Waarde, J.A.; Jansen, P.A. [Hallucinations and vivid dreams by use of metoprolol]. *Tijdschr. Psychiatr.* **2010**, *52*, 117–121. [PubMed]

66. Westerlund, A. Central nervous system side-effects with hydrophilic and lipophilic beta-blockers. *Eur. J. Clin. Pharmacol.* **1985**, *28*, 73–76. [CrossRef]

67. Neil-Dwyer, G. The clinical importance of lipid solubility in beta blockers. *Aviat. Space Environ. Med.* **1981**, *52*, S19–S22.

68. Evans, A.K.; Ardestani, P.M.; Yi, B.; Park, H.H.; Lam, R.K.; Shamloo, M. Beta-adrenergic receptor antagonism is proinflammatory and exacerbates neuroinflammation in a mouse model of Alzheimer's Disease. *Neurobiol. Dis.* **2020**, *146*, 105089. [CrossRef]

69. Laurens, C.; Abot, A.; Delarue, A.; Knauf, C. Central Effects of Beta-Blockers May Be Due to Nitric Oxide and Hydrogen Peroxide Release Independently of Their Ability to Cross the Blood-Brain Barrier. *Front. Neurosci.* **2019**, *13*, 33. [CrossRef]

70. Coyle, C.H.; Martinez, L.J.; Coleman, M.C.; Spitz, D.R.; Weintraub, N.L.; Kader, K.N. Mechanisms of H2O2-induced oxidative stress in endothelial cells. *Free Radic. Biol. Med.* **2006**, *40*, 2206–2213. [CrossRef]

71. Xu, L.; Korade, Z.; Rosado, J.D.A.; Liu, W.; Lamberson, C.R.; Porter, N.A. An oxysterol biomarker for 7-dehydrocholesterol oxidation in cell/mouse models for Smith-Lemli-Opitz syndrome. *J. Lipid Res.* **2011**, *52*, 1222–1233. [CrossRef]

72. Duc, D.; Vigne, S.; Pot, C. Oxysterols in Autoimmunity. *Int. J. Mol. Sci.* **2019**, *20*, 4522. [CrossRef]

73. Koella, W.P. CNS-related (side-)effects of beta-blockers with special reference to mechanisms of action. *Eur. J. Clin. Pharmacol.* **1985**, *28*, 55–63. [CrossRef] [PubMed]

74. Kostis, J.B.; Rosen, R.C. Central nervous system effects of beta-adrenergic-blocking drugs: The role of ancillary properties. *Circulation* **1987**, *75*, 204–212. [CrossRef] [PubMed]

75. Muller, G.; Lubow, C.; Weindl, G. Lysosomotropic beta blockers induce oxidative stress and IL23A production in Langerhans cells. *Autophagy* **2020**, *16*, 1380–1395. [CrossRef] [PubMed]

76. Oliver, E.; Mayor, F., Jr.; D'Ocon, P. Beta-blockers: Historical Perspective and Mechanisms of Action. *Rev. Esp. Cardiol. (Engl. Ed.)* **2019**, *72*, 853–862. [CrossRef]

77. Yoshida, H.; Suzukawa, M.; Ishikawa, T.; Shige, H.; Nishio, E.; Hosoai, H.; Ayaori, M.; Nakamura, H. Effects of beta-blockers on HMG CoA reductase and LDL receptor activity in cultured human skin fibroblasts. *Cardiovasc. Drugs Ther.* **1996**, *10*, 67–74. [CrossRef]

78. Ruys, T.P.; Maggioni, A.; Johnson, M.R.; Sliwa, K.; Tavazzi, L.; Schwerzmann, M.; Nihoyannopoulos, P.; Kozelj, M.; Marelli, A.; Elkayam, U.; et al. Cardiac medication during pregnancy, data from the ROPAC. *Int. J. Cardiol.* **2014**, *177*, 124–128. [CrossRef]

79. Eroli, F.; Johnell, K.; Latorre-Leal, M.; Hilmer, S.; Wastesson, J.; Cedazo-Minguez, A.; Maioli, S. Long-term exposure to polypharmacy impairs cognitive functions in young adult female mice. *Aging (Albany NY)* **2021**, *13*, 14729–14744. [CrossRef]

80. Siwek, M.; Woron, J.; Gorostowicz, A.; Wordliczek, J. Adverse effects of interactions between antipsychotics and medications used in the treatment of cardiovascular disorders. *Pharmacol. Rep.* **2020**, *72*, 350–359. [CrossRef]

81. Pringsheim, T.; Gardner, D.; Addington, D.; Martino, D.; Morgante, F.; Ricciardi, L.; Poole, N.; Remington, G.; Edwards, M.; Carson, A.; et al. The Assessment and Treatment of Antipsychotic-Induced Akathisia. *Can. J. Psychiatry* **2018**, *63*, 719–729. [CrossRef]

82. Salem, H.; Nagpal, C.; Pigott, T.; Teixeira, A.L. Revisiting Antipsychotic-induced Akathisia: Current Issues and Prospective Challenges. *Curr. Neuropharmacol.* **2017**, *15*, 789–798. [CrossRef]

83. Adler, L.A.; Angrist, B.; Rotrosen, J. Metoprolol versus propranolol. *Biol. Psychiatry* **1990**, *27*, 673–675. [CrossRef]

84. Genaro-Mattos, T.C.; Tallman, K.A.; Allen, L.B.; Anderson, A.; Mirnics, K.; Korade, Z.; Porter, N.A. Dichlorophenyl piperazines, including a recently-approved atypical antipsychotic, are potent inhibitors of DHCR7, the last enzyme in cholesterol biosynthesis. *Toxicol. Appl. Pharmacol.* **2018**, *349*, 21–28. [CrossRef] [PubMed]

85. Balog, M.; Anderson, A.; Genaro-Mattos, T.C.; Korade, Z.; Mirnics, K. Individual and simultaneous treatment with antipsychotic aripiprazole and antidepressant trazodone inhibit sterol biosynthesis in the adult brain. *J. Lipid Res.* **2022**, *63*, 100249. [CrossRef] [PubMed]

86. Genaro-Mattos, T.C.; Anderson, A.; Allen, L.B.; Korade, Z.; Mirnics, K. Altered Cholesterol Biosynthesis Affects Drug Metabolism. *ACS Omega* **2021**, *6*, 5490–5498. [CrossRef] [PubMed]

87. Korade, Z.; Genaro-Mattos, T.C.; Tallman, K.A.; Liu, W.; Garbett, K.A.; Koczok, K.; Balogh, I.; Mirnics, K.; Porter, N.A. Vulnerability of DHCR7(+/-) mutation carriers to aripiprazole and trazodone exposure. *J. Lipid Res.* **2017**, *58*, 2139–2146. [CrossRef] [PubMed]

88. Shariq, O.A.; McKenzie, T.J. Obesity-related hypertension: A review of pathophysiology, management, and the role of metabolic surgery. *Gland Surg.* **2020**, *9*, 80–93. [CrossRef]

89. Fantin, F.; Giani, A.; Zoico, E.; Rossi, A.P.; Mazzali, G.; Zamboni, M. Weight Loss and Hypertension in Obese Subjects. *Nutrients* **2019**, *11*, 1667. [CrossRef]

90. Re, R.N. Obesity-related hypertension. *Ochsner. J.* **2009**, *9*, 133–136.

91. Mikhail, N.; Golub, M.S.; Tuck, M.L. Obesity and hypertension. *Prog. Cardiovasc. Dis.* **1999**, *42*, 39–58. [CrossRef]

92. Powell-Wiley, T.M.; Poirier, P.; Burke, L.E.; Despres, J.P.; Gordon-Larsen, P.; Lavie, C.J.; Lear, S.A.; Ndumele, C.E.; Neeland, I.J.; Sanders, P.; et al. Obesity and Cardiovascular Disease: A Scientific Statement From the American Heart Association. *Circulation* **2021**, *143*, e984–e1010. [CrossRef]

93. Mandviwala, T.; Khalid, U.; Deswal, A. Obesity and Cardiovascular Disease: A Risk Factor or a Risk Marker? *Curr. Atheroscler. Rep.* **2016**, *18*, 21. [CrossRef] [PubMed]

94. Meldrum, D.R.; Morris, M.A.; Gambone, J.C. Obesity pandemic: Causes, consequences, and solutions-but do we have the will? *Fertil. Steril.* **2017**, *107*, 833–839. [CrossRef] [PubMed]

95. Swinburn, B.A.; Sacks, G.; Hall, K.D.; McPherson, K.; Finegood, D.T.; Moodie, M.L.; Gortmaker, S.L. The global obesity pandemic: Shaped by global drivers and local environments. *Lancet* **2011**, *378*, 804–814. [CrossRef]

96. Kelley, R.I. Diagnosis of Smith-Lemli-Opitz syndrome by gas chromatography/mass spectrometry of 7-dehydrocholesterol in plasma, amniotic fluid and cultured skin fibroblasts. *Clin. Chim. Acta* **1995**, *236*, 45–58. [CrossRef]

97. Cross, J.L.; Iben, J.; Simpson, C.L.; Thurm, A.; Swedo, S.; Tierney, E.; Bailey-Wilson, J.E.; Biesecker, L.G.; Porter, F.D.; Wassif, C.A. Determination of the allelic frequency in Smith-Lemli-Opitz syndrome by analysis of massively parallel sequencing data sets. *Clin. Genet.* **2015**, *87*, 570–575. [CrossRef]